Received: 17 July 2016 | Revised: 13 January 2017 | Accepted: 16 January 2017

DOI 10.1002/cne.24178

RESEARCH ARTICLE

WILEY The Journal of Comparative Neurology

White matter atrophy and myelinated fiber disruption in a rat model of depression

Yuan Gao [1,2,3*] | Jing Ma[2,3*] | Jing Tang[2,3] | Xin Liang[2,3] | Chun-Xia Huang[2,3,4] | San-rong Wang[2,3] | Lin-mu Chen[2,3] | Fei-Fei Wang[2,3] | Chuan-Xue Tan[2,3] | Feng-Lei Chao[2,3] | Lei Zhang[2,3] | Xuan Qiu[2,3] | Yan-Min Luo[2,3] | Qian Xiao[2,3] | Lian Du[2,3,5] | Qian Xiao[1] | Yong Tang[2,3]

[1]Department of Geriatrics, The First Affiliated Hospital, Chongqing Medical University, Chongqing, P. R. China

[2]Department of Histology and Embryology, Chongqing Medical University, Chongqing, P. R. China

[3]Laboratory of Stem Cells and Tissue Engineering, Faculty of Basic Medical Sciences, Chongqing Medical University, Chongqing, P. R. China

[4]Department of Physiology, Chongqing Medical University, Chongqing, P. R. China

[5]Department of Psychiatry, The First Affiliated Hospital, Chongqing Medical University, Chongqing, P. R. China

Correspondence
Yong Tang, Department of Histology and Embryology, Faculty of Basic Medical Sciences, Chongqing Medical University, Chongqing, P. R. China.
Email: ytang062@163.com

Abstract

Brain imaging and postmortem studies have indicated that white matter abnormalities may contribute to the pathology and pathogenesis of depression. However, until now, no study has quantitatively investigated white matter changes in depression in rats. The current study used the chronic unpredictable stress (CUS) model of depression. Body weight and sucrose preference test (SPT) scores were assessed weekly. Upon successfully establishing the CUS animal model, all animals were tested using the SPT and the open field test (OFT). Then, transmission electron microscopy and unbiased stereological methods were used to investigate white matter changes in the rats. Compared with the control group, the body weight and sucrose preference of the CUS rats were significantly decreased ($p < .001$, $p < .001$, respectively). In the OFT, the total time spent and the total distance traveled in the inner area by the CUS rats were significantly lower than those of the control group ($p = .002$, $p = .001$, respectively). The stereological results revealed that white matter volume, the total volume, and the total length and mean diameter of myelinated fibers in the white matter of the CUS rats were significantly decreased compared to the control rats ($p = .042$, $p = .038$, $p = .035$, $p = .019$, respectively). The results of this study suggested that white matter atrophy and disruption of myelinated fibers in the white matter may contribute to the pathophysiology underlying depression, which might provide new targets for the development of novel therapeutic interventions for depression.

KEYWORDS

chronic unpredictable stress, depression, myelinated fibers, stereology, white matter, RRID: AB_956157, RRID: SCR_002526

1 | INTRODUCTION

The monoaminergic hypothesis of depression posits that depression is caused by decreased monoamine function in the brain (Berton & Nestler, 2006). In clinical practice, monoamine-based antidepressants remain the first-line therapy for depression. Although antidepressants induce a rapid increase in the intrasynaptic levels of serotonin and/or norepinephrine, the onset of an appreciable clinical effect usually takes at least 3 to 4 weeks (Duman, Malberg, Nakagawa, & D'Sa, 2000; Manji, Drevets, & Charney, 2001; Wong & Licinio, 2001), which indicates that structural changes might occur within the depressed brain (Pittenger & Duman, 2008). This realization provides a strong impetus to search beyond monoaminergic systems to develop a better understanding of the neurobiology of depression and to consider these newly identified mechanisms in the search for novel antidepressant treatments (Berton & Nestler, 2006; Drevets, Price, & Furey, 2008; Manji et al., 2003)

Regarding structural changes in the depressed brain, several lines of evidence have indicated that white matter abnormalities may play a vital role in the pathophysiological mechanisms underlying depression.

*Yuan Gao and Jing Ma are co-first authors.

TABLE 1 Schedule of CUS stressors

Time	Sunday	Monday	Tuesday	Wednesday	Thursday	Friday	Saturday
Week 1	Tail pinch, restraint	Water deprivation	Wet bedding	Hot stress	Tail pinch, cage tilt, lights on/off,	Lights on/off, food and water deprivation	**SPT**
Week 2	Cold stress	Restraint	Lights on/off, cage tilt	Lights on/off, cage tilt, water deprivation, wet bedding	Cold stress	Food and water deprivation	**SPT**
Week 3	Lights on/off, cage tilt	Hot stress	Lights on/off, cage tilt	Restraint	Cold stress	Lights on/off, tail pinch	**SPT**
Week 4	Hot stress, wet bedding	Restraint	Lights on/off	Cage tilt	Food and water deprivation	**OFT**	**SPT**

SPT = sucrose preference test; OFT = open field test

Previous structural magnetic resonance imaging (MRI) studies demonstrated smaller white matter volumes in diverse brain regions in depression, including the whole brain, the prefrontal cortex, the medial temporal lobe, the hippocampus, and the corpus callosum (Ballmaier et al., 2004; Bell-McGinty et al., 2002; Berton & Nestler, 2006; Brambilla et al., 2004; Drevets et al., 2008; Frodl et al., 2008; Hashimoto et al., 2006; Manji et al., 2003; Steingard et al., 2002). Previous diffusion tensor imaging (DTI) and MRI investigations of depressed brains also showed decreased fractional anisotropy (FA) and increased white matter hyperintensities (WMHs), which indicate white matter lesions (WMLs) (Kieseppa et al., 2010; Ma et al., 2007; Taylor et al., 2004; Tham, Woon, Sum, Lee, & Sim, 2011). In clinical studies, WMLs usually represent demyelination, which is associated with the clinical severity and treatment responsiveness of depression (Iosifescu et al., 2006; Papakostas et al., 2005; Taylor et al., 2004). Therefore, WMLs could serve as diagnostic and treatment indicators in depressed patients (Dalby et al., 2010; Heiden et al., 2005; Kumar et al., 2004; Papakostas et al., 2005; Weber et al., 2010)

Advances in brain imaging techniques have revealed structural and functional white matter changes that are linked to depression. Brain neuroimaging changes, including increased WMHs and decreased FA, only provide a vague view of WMLs. To explore the pathological correlation of white matter imaging changes in depressed brains, this study was designed to quantitatively investigate changes in white matter and in the myelinated fibers in white matter in depressed brains. We hypothesized that white matter changes and myelinated fiber changes in the white matter may be involved in the pathological mechanism underlying depression. White matter and its myelinated fibers are difficult to visualize and quantify, although unbiased stereological techniques have been demonstrated as reliable and objective in quantitative studies of the morphological changes in myelinated fibers in the white matter (Li et al., 2009; Tang, Nyengaard, Pakkenberg, & Gundersen, 1997). Most morphological studies on brain changes in depression have utilized animal models of depression (Willner, Towell, Sampson, Sophokleous, & Muscat, 1987), in which a depressive-like behavioral state is induced in rodents by exposing them to chronic unpredictable stress (CUS) (Willner et al., 1987; Willner, 2005). The rodent CUS model, one of the most valid and relevant models of depression (Willner et al., 1987; Willner, 2005; Banasr & Duman, 2008), consists of long-term, daily exposure of animals to a series of mild and unpredictable stressors designed to prevent habituation (Willner, 2005). In this study, we used the chronic unpredictable stress (CUS) model of depression combined with behavioral tests, electron microscopy techniques and stereological methods to investigate changes in white matter and in the myelinated fibers in the white matter of depressed brains.

2 | MATERIALS AND METHODS

2.1 | Animal housing and chronic unpredictable stress (CUS)

A total of 100 male Sprague-Dawley rats were used in the present study. Adult male Sprague–Dawley rats (10–12 weeks old at the beginning of the CUS exposure) were housed in groups of 5 per cage under a 12-hr light/dark cycle (lights on at 07:00 hr) at constant temperature (22 ± 1 °C) and humidity with free access to food and water. Animals were allowed at least 1 week to habituate to the housing conditions before any experiments were initiated. All animals were age- and weight-matched (rats weighed 250–300 g) at the beginning of the experiments. All rat housing, treatment and maintenance procedures were performed in accordance with the National Institutes of Health Guide for the Care and Use of Laboratory Animals and approved by the Chongqing Medical University Care and Use of Laboratory Animals guidelines.

After the rats were adapted to 1% sucrose, the sucrose preference of the rats was tested using a sucrose preference test (SPT). Only 96 animals that exhibited an initial sucrose preference > 65% were used for further experiments. The 96 rats were chosen and randomly divided into control group ($n = 10$) and model group ($n = 86$). The model group rats were housed with one rat per cage and exposed to four weeks of CUS stimulation. The Model rats were subjected to a sequence of 10 different stressors (one or two per day for 28 consecutive days), including cold stress, hot stress, lights on/off, food, and/or water deprivation, wet bedding, 1-hr restraint, tail pinch and cage tilt. This procedure was adapted from Willner (Willner et al., 1987), Banasr (Banasr et al., 2007) and Seney (Seney, Walsh, Stolakis, & Sibille, 2012; Table 1). After 4 weeks of CUS stimulation, only 17 rats in the model group exhibited

the sucrose preference < 65%. These 17 rats were finally used as the CUS group. The control group rats did not receive any treatments, but they were handled every day. The effects of stress on the hedonic state of the rats were assessed weekly using the SPT and body weight measurements. When the CUS stimulation period was complete, all animals were finally tested using the SPT and the open field test (OFT).

2.2 | Sucrose preference test

All animals were singly caged for the SPT. Rats were presented with two bottles: one bottle was filled with sucrose solution (1%), and the other bottle was filled with water. The bottle containing the sucrose solution was randomly placed on the left or right side of the compartment. During the SPT, the positions of the bottles in the cages are switched often. This procedure was adapted from Willner (Willner et al., 1987) and Banasr (Banasr et al., 2007). Sucrose and water consumption were determined by measuring the change in each consumed fluid volume. Sucrose preference was defined as the ratio of the volume of sucrose vs water consumed during the 24-hr test. Animals were first trained with both bottles while housed in groups. The animals were individually housed for subsequent tests, including the tests performed during the baseline period. The consumption of water and sucrose was measured by weighing the bottles. Preference for sucrose was calculated as a percentage of consumed sucrose-containing solution relative to the total amount of liquid intake. (Cai et al., 2013; Christianson et al., 2008; Couch et al., 2013).

2.3 | Open field test

All animals were tested on the 28th day of the experimental period using the OFT. This test was conducted as previously described (Xiu et al., 2015). Briefly, the testing apparatus consisted of four Perspex boxes ($50 \times 50 \times 40\,cm^3$) with video devices (RD 1112-OF-M-4, Shanghai Mobil Datum Information Technology Co., China). The animal was placed in the center of the test box, and the movements of the animal were recorded for 5 min. Computer software was used to calculate the velocity, the total distance traveled, and the distance and the time spent in the center zone. These parameters reflect locomotor activity and anxiety, respectively. After each trial, the apparatus was cleaned with a water solution containing 70% ethanol to prevent any olfactory-induced behavioral modifications.

2.4 | Protein extraction and western blotting

Lysates were generated using RIPA Lysis buffer (Beyotime) supplemented with 1% protease inhibitor phenylmethanesulfonyl fluoride (vol/vol, Beyotime). Protein concentration was determined using a Thermo BCA Protein Assay Kit (Beyotime) according to the manufacturer's instructions. Samples were heated at 100 °C for 10 min, and 10 μg total protein was loaded onto 10% acrylamide gels. Then, proteins were transferred onto polyvinylidene difluoride (PVDF) membranes (Millipore) for 40 min and separated at 210 mA in transfer buffer. Membranes were blocked with 5% powdered milk in Tris-buffered saline (TBST) for 2 hr at room temperature on an orbital shaker. The membranes were then incubated with the primary antibody overnight at 4 °C, washed thrice in TBST for 5 min, and incubated with horseradish peroxidase (HRP)-conjugated IgG secondary antibody for 2 hr at room temperature. Chemiluminescent substrate detection reagent (Pierce ECL Western Blotting Substrate, Beyotime) was used, and autoradiography film processing was performed, followed by analysis with Image Lab (Bio-Rad).

2.5 | Stereological methods

2.5.1 | Tissue preparation

In this study, six rats were randomly selected from each group and used for stereological analyses. The animals were anaesthetized by injection of 1% pentobarbital sodium intraperitoneally (0.4 mL/100 g) and then perfusion-fixed with 2% paraformaldehyde and 2.5% glutaraldehyde in 0.1 M phosphate-buffered saline (pH 7.4). After each animal was perfusion-fixed, the cerebrum, meninges, cerebellum, and brain stem were removed. The right or left hemisphere was chosen at random beforehand. The hemispheres were embedded in 6% agar and sliced coronally in 1-mm wide sections starting randomly at the rostral pole. An average of 17 sections were obtained from each hemisphere.

2.6 | Estimation of white matter volume

The total white matter volume of the 1-mm-thick tissue blocks was measured using Cavalieri's principle (Tang & Nyengaard, 1997; Tang et al., 1997). A transparent plastic counting grid with an area of $0.19\,mm^2$ per point was placed at random on all brain slabs containing white matter (Figure 1). The points hitting the white matter were counted under an anatomical microscope at an approximate magnification of ×10. The white matter boundary in each slab was identified according to Paxinos (Papakostas et al., 2005), and the white matter volume, V (mw), was calculated using Cavalieri's principle (Gundersen et al., 1988; Tang et al., 1997). An average of 304 points overlapping white matter were counted per rat.

2.7 | Random sampling of the white matter and tissue processing for electron microscopy sections

Six rats from each group were randomly selected for electron microscopy. From the sections of the extracted hemisphere, the first slab was randomly selected, and then every second section was systematically analyzed. A plastic sheet with equidistantly points (1 mm × 1 mm) was placed over the section. Tissue blocks of approximately $1\,mm^3$ were sampled where the points on the sheet overlapped white matter. If more than 2 points overlapped white matter in a slab, an additional point was randomly sampled. An average of five tissue blocks were sampled per rat and were used for the further stereological estimations. This sampling technique ensured that the final samples represented all parts of the white matter. Then, the sections were postfixed in 4% glutaraldehyde for at least 2 hr at 4 °C, rinsed in 0.1 M phosphate-buffered saline three times, and osmicated in 1% 0.1 M phosphate-buffered osmium tetroxide at 4 °C for 2 hr. The blocks were

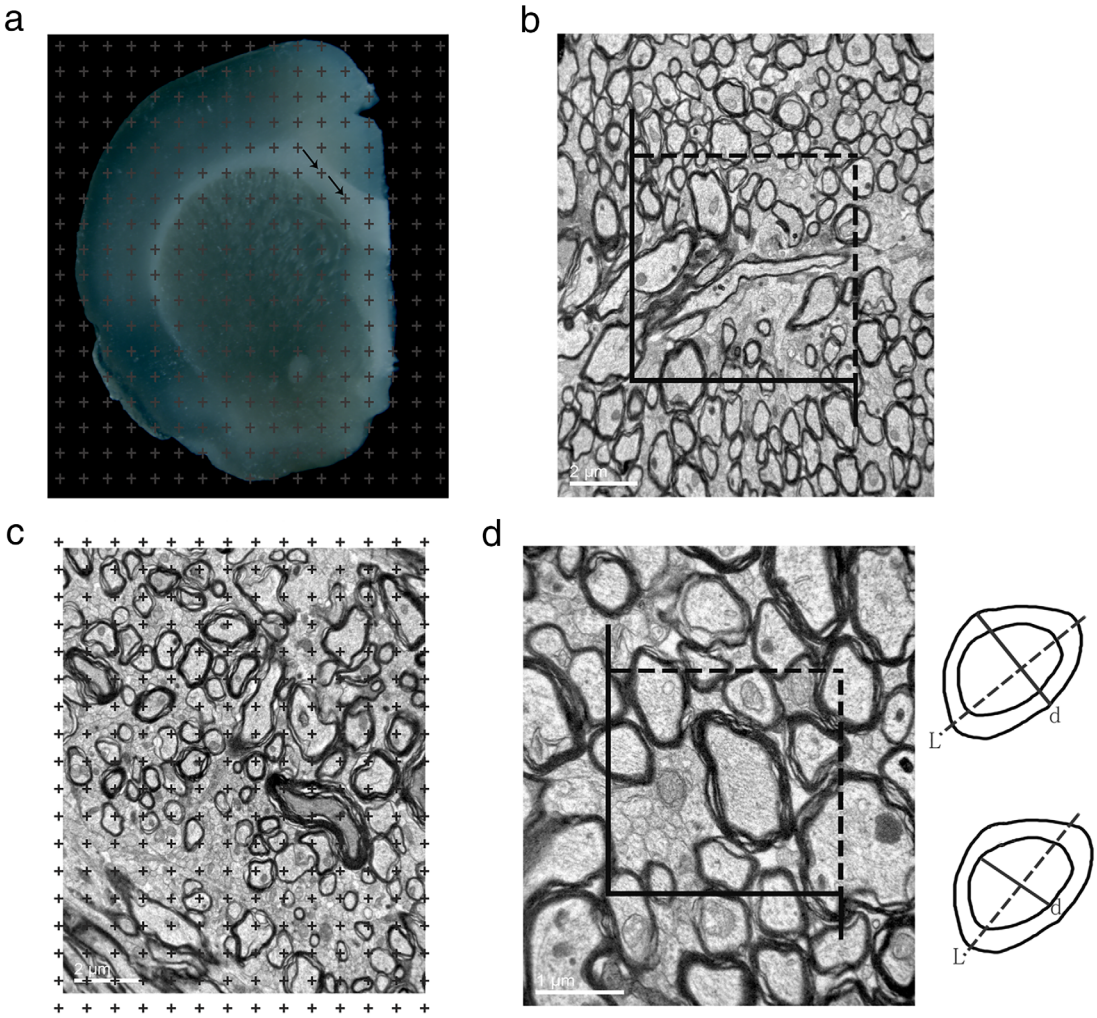

FIGURE 1 (a) A rat brain section images using an anatomic microscope is shown. A point grid was superimposed on the section, and the points hitting the white matter were counted, as indicated by the arrows. (b) The principle of an unbiased counting frame: all nerve fiber profiles inside the counting frame that do not hit or intersect the solid lines are considered for counting. Bar = 2 μm. (c) The number of points hitting the white matter, the number of points hitting the myelinated fibers and the number of points hitting the myelin sheaths are counted. Bar = 2 μm. (d) Left: all myelinated fiber profiles completely inside the counting frame or partly inside the frame but not hitting or intersecting the solid lines were sampled for estimation. Right upper: The outer diameters (d) of the myelinated fibers sampled using an unbiased counting frame were estimated by measuring the longest myelinated fiber profile diameter perpendicular to its longest axis (L). Right lower: The inner diameters (d) of the myelinated fibers sampled using the unbiased counting frame were estimated by measuring the longest axonal profile diameter perpendicular to its longest axis (L). Bar = 1 μm

gradually dehydrated through a series of 50, 70, and 90% ethanol followed by a 90% ethanol and 90% acetone mixture, and finally 100% acetone. Then, the blocks were infiltrated with epoxy resin 618 at an acetone:resin ratio of 1:1 (3 hr at room temperature) and then infiltrated with absolute resin (2 hr at 37 °C). In this study, the tissue blocks were embedded in 5-mm EPON spheres. After the spheres had hardened, they were rotated randomly before being re-embedded in an oven at 37 °C for 16 hr, 45 °C for 12 hr, and finally 60 °C for 14 hr. This procedure, known as isector (Nyengaard & Gundersen, 1992), ensures that isotropic, uniform and random sections are generated so that each tissue sample has a uniform random orientation before being cut. This approach is essential for unbiased estimation of myelinated fiber length to avoid methodological bias due to the anisotropic orientation of the myelinated fibers. One 60-nm-thick section was obtained from the center of each EPON block using an ultramicrotome. The ultrathin sections were then viewed using a transmission electron microscope (Hitachi-7500, made by Hitachi, Ltd., Japan). From each section, eight fields of view were randomly imaged at 8,000 × magnification.

2.8 | Estimations of the length density and total length of the myelinated fibers in the white matter

An unbiased counting frame (Gundersen, 1977) with an area of 6,000 mm^2 was overlaid on the captured images. The myelinated fiber profiles inside the counting frame or hitting the top or right dotted lines (inclusion lines) were included for counting, whereas any fibers hitting the left solid line or the bottom solid line and the extensions of the right and left solid lines (exclusion lines) were not counted (Figure 1b).

The length density of the myelinated fibers in the white matter, L_V (mf/wm), was estimated as described previously (Li et al., 2009; Tang & Nyengaard, 1997; Tang et al., 1997). The total length of the myelinated fibers in the white matter, L (mf, wm), was estimated as L_V (mf/wm) × V (wm) (Li et al., 2009; Tang & Nyengaard, 1997; Tang et al., 1997). An average of 335 myelinated fiber profiles were counted at low magnification (×8,000) in the white matter per rat.

2.9 | Estimations of the volume densities and total volumes of the myelinated fibers, axons, and myelin sheaths in the white matter

A transparent counting grid with 315 total points was placed on the captured images (Figure 1c). The points hitting myelinated fibers, ∑P (mf); the points hitting the axons, ∑P(ma); the points hitting the myelin sheaths, ∑P(ms); and the points hitting the white matter, ∑P(wm), were separately counted. The volume density of the myelinated fibers, V_V(mf/wm); the volume density of the axons, V_V(ma/wm); and the volume density of the myelin sheaths, V_V(ms/wm), in the white matter were estimated as described previously (Li et al., 2009; Tang & Nyengaard, 1997; Tang et al., 1997). An average of 12,600 points hit white matter, 8,195 points hit myelinated fibers, 2465 points hit myelin sheaths, and 5,730 points hit myelinated axons at low magnification (×8,000) in the white matter per rat.

2.10 | Estimation of the mean diameter of the myelinated fibers in the white matter

To estimate the mean diameter of the myelinated fibers in the white matter, twelve fields of view were randomly imaged from each section at 20,000× magnification. The external diameter of the myelinated fibers was derived by measuring its longest profile diameter perpendicular to the longest axis of the myelinated fibers, and measurements were obtained from the outer limit of the myelin sheath (Figure 1d). The internal diameter of the myelinated fibers was estimated by measuring the longest profile diameter perpendicular to the longest axis of the axon (Figure 1d).

2.11 | Estimation of the mean perimeter of myelin sheath cross-sections in the white matter

Using the randomly captured images of the sections, estimates of the inner and outer perimeters of the myelin sheaths were obtained by superimposing a grid of parallel lines on the profiles and sampling using an unbiased counting frame (Figure 1d). The number of intersections between the profile boundary and the test lines, I, was counted. The inner or outer perimeter estimate, b(ms), was calculated as described previously (Li et al., 2009; Tang & Nyengaard, 1997; Tang et al., 1997).

The inner perimeter of the myelin sheaths was calculated when the intersections between the inner boundary of myelin sheaths and the test lines were counted. The outer perimeter of myelin sheaths was calculated when the intersections between the outer boundary of myelin sheaths and the test lines were counted. It should be emphasized that the perimeter measures were not obtained using the unbiased stereological sampling method in three-dimensions.

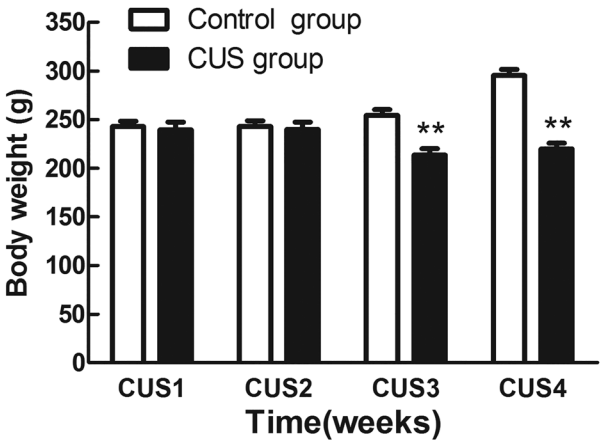

FIGURE 2 Column chart of body weight (mean ± SEM) of rats in the control group ($n = 10$) and the CUS group ($n = 17$). ** indicates $p < .01$ compared to the control group

2.12 | Tissue shrinkage

We observed an 11.46% volume shrinkage due to electron microscopy processing (Yang et al., 2009). As the shrinkage, did not differ between the groups, we did not correct for this minor and constant shrinkage in our results.

2.13 | Statistical analyses

Statistical analyses were performed using SPSS (ver. 19.0, SPSS Inc., Chicago, USA). The behavioral sucrose preference test scores, body weight and open field test scores are presented as the mean ± standard error of the mean (SEM). The other results are presented as the mean ± standard deviation (SD). The effects of CUS on sucrose preference and body weight were analyzed using repeated measures ANOVA. Student's *t*-tests were used to compare the other results between the two groups. Two-tailed Student's tests were used when normality assumptions were satisfied. Otherwise, unpaired Mann-Whitney *U* tests were used to compare the relevant group means. The level of statistical significance was set at $p < .05$.

3 | RESULTS

3.1 | Effects of CUS on behavior

After the four-week CUS procedure, the CUS animals lost weight, while the control animals remained stable ($p < .001$, Figure 2). In addition, sucrose preference of the depressed rats was significantly decreased compared to the control rats ($p < .001$, Figure 3). In the OFT, the total distance traveled and the mean speed of the CUS group did not differ from those of the control group ($p = .164$, $p = .164$; Figure 4a,b). The distance traveled in the inner area by the CUS group was significantly decreased compared to the distance traveled by the

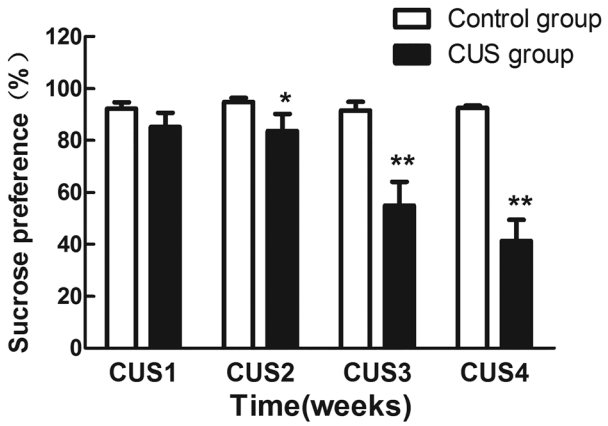

FIGURE 3 Sucrose preference changes (mean ± SEM) in the control group ($n = 10$) and the CUS group ($n = 17$). * indicates $p < .05$ compared to the control group; ** indicates $p < .01$ compared to the control group

control group ($p = .002$; Figure 4c). For the CUS group, the percentage of time spent in the inner area and the percentage of the distance traveled in the inner area were significantly decreased compared to the control group ($p = .002$ and $p = .001$, respectively; Figure 4d).

3.2 | CUS-induced demyelination in the white matter

The myelin basic protein (MBP) level in the white matter between the control group and the CUS group were analyzed using western blotting (Figure 5a). The expression of MBP in the white matter of the CUS rats was significantly decreased compared to the control rats ($p = .012$, Figure 5b). Ultrastructural analysis further revealed that the myelin sheath integrity was compromised in the CUS rats (Figure 5c–f).

3.3 | Stereological results of CUS on white matter and myelinated fibers in the white matter

All coefficient of error (CE), except those for the myelinated fiber length in the CUS group, were below the recommended values (Table 2).

The mean white matter volumes in the CUS rats and the control rats were $53.39 \pm 10.08\,mm^3$ (mean ± SD) and $67.71 \pm 11.19\,mm^3$ (Table 2, Figure 6). The white matter volume in the CUS rats was significantly decreased compared to that in the control rats ($p = .042$; Table 2, Figure 6). The total volume of the myelinated fibers in the white matter of the CUS rats ($31.78 \pm 6.58\,mm^3$) was significantly decreased compared to that of the control rats ($41.77 \pm 7.77\,mm^3$; $p = 0.038$; Table 2, Figure 7a). The total length of the myelinated fibers in the white matter in the CUS rats (49.68 ± 18.30 km) was significantly

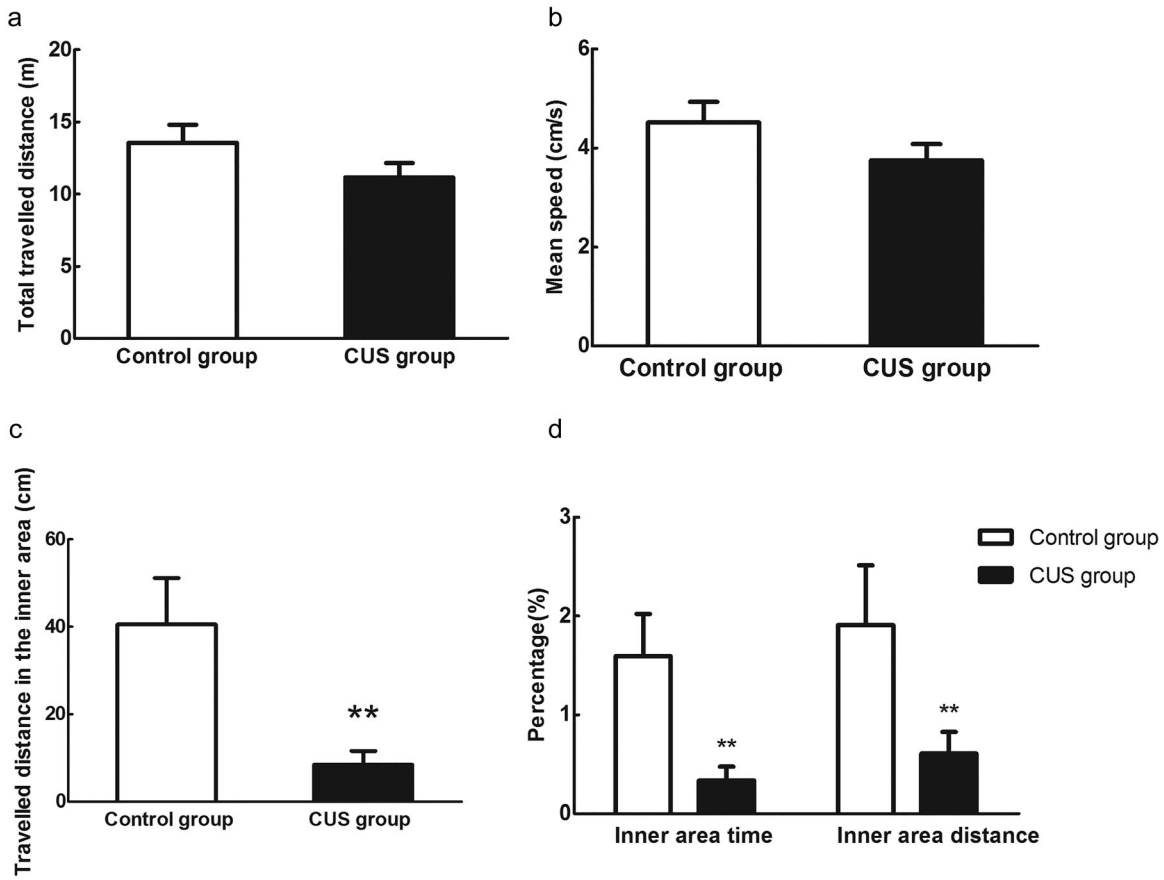

FIGURE 4 OFT results (mean ± SEM) of the control group ($n = 10$) and the CUS group ($n = 17$). a. Total distance traveled in 5 min in the open field area. b. Mean speed of travel in the open field area. c. Distance traveled in 5 min in the inner area. d. The percentage of time spent in the inner area and the percentage of the distance traveled in the inner area. ** indicates $p < .01$ compared to the control group

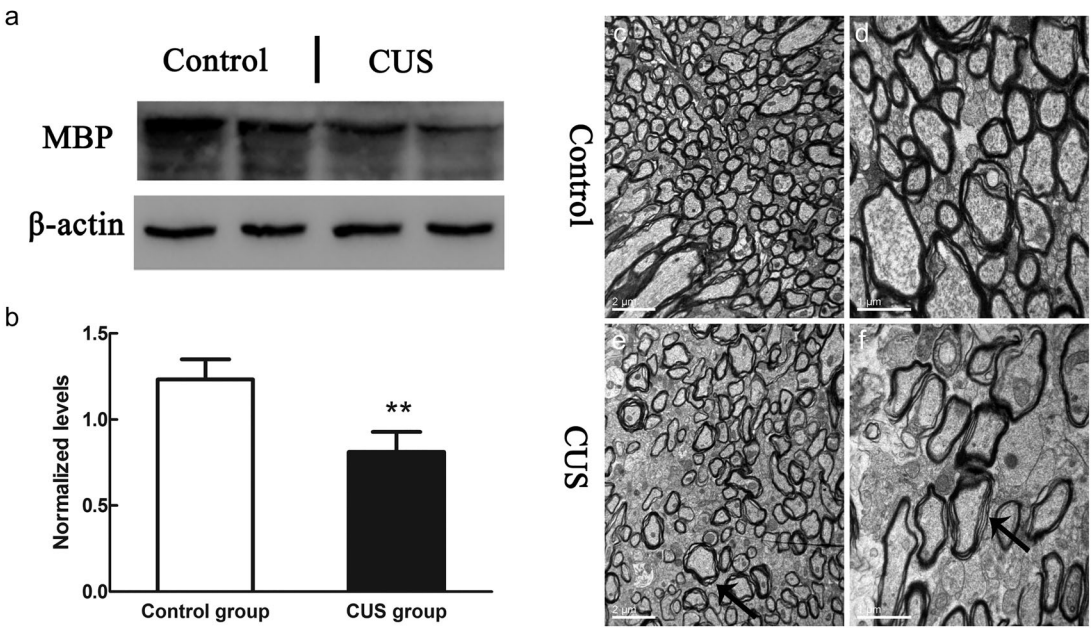

FIGURE 5 CUS-induced demyelination in the white matter. (a,b) Western blot analysis of white matter using an antibody for MBP. Data are shown as the mean ± SD (n = 6 rats per group). Ultrastructural changes in myelinated nerve fibers in the control group and the CUS group. (c,d) Myelin sheaths at magnifications of 8,000 × (Bar = 2 μm) and 20,000 × (Bar = 1 μm) in the control group. (e,f) Myelin sheaths at magnifications of 8,000 × and 20,000 × in the CUS group. The myelin staining intensity decreased, the myelin sheaths exhibited edema, and the layers of the myelin sheaths became disordered, thick, and even broke down in the CUS group compared to the control group (black arrow head)

decreased by compared to that of the control rats (72.33 ± 12.80 km; $p = .035$; Table 2, Figure 7b). The total volume of the axons of the myelinated fibers in the white matter of the CUS rats (17.09 ± 3.74 mm^3) was significantly decreased compared to that of the control rats (23.83 ± 4.50 mm^3; $p = .019$; Table 2, Figure 7c). However, the total volume of the myelin sheaths in the white matter of the CUS rats

TABLE 2 Stereological estimates of myelinated fibers in the white matter

	Control group Mean(CV)	Control group CE (%)	CUS group Mean(CV)	CUS group CE (%)	*p*
V(wm) (mm^3)	67.71(0.17)	0.95	53.39(0.19) *	1.2	0.04
V_V(mf)	0.62(0.07)	5.15	0.60(0.09)	4.38	0.50
V(mf) (mm^3)	41.77(0.19)	5.24	31.78(0.21)*	4.56	0.04
V_V(ms)	0.26(0.08)	8.43	0.28(0.08)	7.43	0.37
V(ms) (mm^3)	17.94(0.19)	8.48	14.69(0.20)	7.54	0.11
V_V(ma)	0.35(0.10)	5.46	0.32(0.11)	4.03	0.16
V(ma) (mm^3)	23.83(0.19)	5.55	17.09(0.22)*	4.22	0.02
L_V(mf) (km/mm^3)	1080.36 (0.17)	14.18	916.41 (0.21)	20.38	0.16
L(mf) (km)	72.33(0.18)	14.21	49.68(0.37)*	20.42	0.03
D(mf) (μm)	0.69(0.04)	1.72	0.64(0.06)*	2.28	0.04
D(a) (μm)	0.47(0.04)	1.81	0.44(0.05)	2.08	0.11
Ob(ms) (μm)	3.50(0.09)	3.49	3.33(0.15)	6.11	0.47
Ib(ms) (μm)	2.55(0.09)	3.52	2.36(0.13)	5.37	0.06

CV = coefficient of variation; CE = coefficient of error; V(wm) = mean volume of the white matter; V_V(mf) = volume density of myelinated nerve fibers; V(mf) = total volume of myelinated fibers; V_V(ms) = volume density of the myelin sheaths; V(ms) = total volume of myelin sheaths; V_V(ma) = volume density of the axons; V(ma) = total volume of axons; L_V(mf) = length density of myelinated fibers; L(mf) = total length of myelinated fibers; D(mf) = mean diameter of nerve fibers; D(a) = mean diameter of axons; Ob(ms) = outer perimeter of myelin sheaths; Ib(ms) = inner perimeter of myelin sheaths.

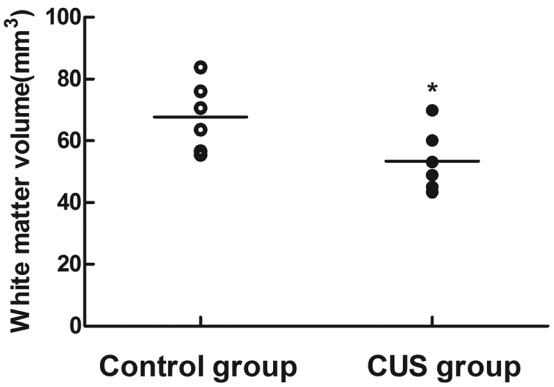

FIGURE 6 Comparison of white matter volume between the control group ($n = 6$) and the CUS group ($n = 6$). * indicates $p < .05$ compared to the control group

($14.69 \pm 2.92\,mm^3$) did not differ from that of the control rats ($17.94 \pm 3.46\,mm^3$; $p = .11$; Table 2, Figure 7d). In addition, the mean diameter of the myelinated fibers in the CUS rats was significantly smaller than that in the control rats (Table 2). However, the inner perimeter, the outer perimeter of the myelin sheaths of the CUS rats were not significantly different compared to those of the control rats ($p = .06$).

4 | DISCUSSION

Depression results from interactions between genetic predisposition and environmental factors, such as chronic stress. The results of chronic stress conditions have been previously observed in studies that have utilized several types of behavioral tests, many of which induce relevant clinically observed symptoms, notably anhedonia (Krishnan et al., 2007; Willner, 2005). Such depressed animals can mimic the typical clinical symptoms of patients with depression, such as anhedonia, agitation or slowed motor activity, helplessness, sleep disorders and decreased social interaction (Berton & Nestler, 2006; Willner et al., 1987). Many of these phenotypes can be reversed by chronic antidepressants (Bondi, Rodriguez, Gould, Frazer, & Morilak, 2008; Strekalova, Gorenkova, Schunk, Dolgov, & Bartsch, 2006). The results of the current study showed that chronic stress induced a robust depressive-like phenotype in SD rats, as evidenced by weight loss and appetite loss. CUS has been reported to decrease sucrose preference, a measure

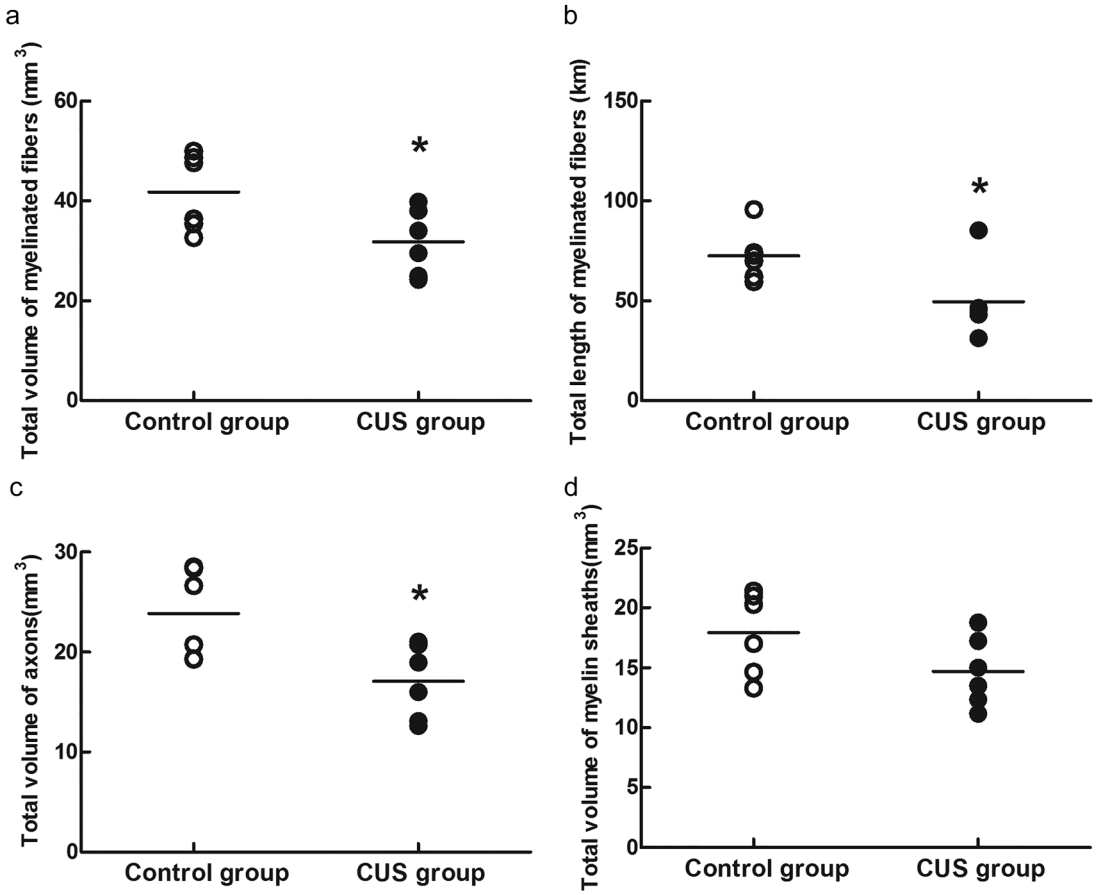

FIGURE 7 (a) Comparison of the total volume of the myelinated fibers in the white matter between the control group ($n = 6$) and the CUS group ($n = 6$). (b) Comparison of the total length of the myelinated fibers in the white matter between the control group ($n = 6$) and the CUS group ($n = 6$). (c) Comparison of the total volume of the axons in the white matter between the control group ($n = 6$) and the CUS group ($n = 6$). (d) Comparison of the total volume of the myelin sheaths in the white matter between the control group ($n = 6$) and the CUS group ($n = 6$). * indicates $p < .05$ compared to the control group

of anhedonia, which is a core symptom of depression. In this study, we also found that CUS decreased the consumption of a sucrose solution relative to water intake, which is consistent with previously reported observations. In the OFT, our results revealed that the CUS rats exhibited significantly decreased activity in the inner area of the box compared to the control rats, and this decrease in activity was interpreted as an anxiety-like behavior. A similar decrease in locomotor activity was observed by measuring the total distance traveled in the OFT; this decrease was considered to reflect diminished activity, which is also a hallmark feature of depression. Therefore, the results of this study further indicated that the rodent model of depression induced by CUS is a valid model for investigating the pathogenesis of depression.

In this study, animals were subjected to a sequence of different stressors for four weeks. Stressful events are thought to constitute "acquired factors" that interact with genetic susceptibility during the development of mood disorders; however, once the illness has been instantiated, the potential links between stressors and subsequent depression become progressively less evident (Krishnan & Nestler, 2008). Previous rodent studies have provided evidence of changes in cellular architecture and/or morphology within several brain regions in response to stress, including alterations of the volumes of the prefrontal cortex, the hippocampus, and the amygdala (Drevets, 2003; Neumeister et al., 2005; Sheline, Price, et al., 2008; Sheline, Wang et al., 1996), atrophy of dendrites and synapses, and decreased cell proliferation and neurogenesis in the hippocampus and cortical areas (Banasr et al., 2007; Czeh et al., 2001; Magarinos, Deslandes, & McEwen, 1999; McEwen, 2000; Santarelli et al., 2003; Schmidt & Duman, 2007). Profound neuroplastic changes have been demonstrated in various structures after chronic stress exposure in animal models of mood disorders. However, no study has investigated the changes in white matter in animal models of depression. In this study, rats were subjected to unpredictable stress daily for 4 weeks, and a stress-induced decrease in white matter volume was observed. This preclinical finding is consistent with previous clinical studies that have demonstrated a decrease in white matter volume in depressed patients, especially in patients with a longer course of illness, more severe clinical parameters and multiple episodes (Duman, Heninger, & Nestler, 1997; Ballmaier et al., 2004; Brambilla et al., 2004; Hashimoto et al., 2006). However, other studies have shown a lack of significant changes in white matter volume in patients with short-term depression and mild clinical symptoms (Abe et al., 2010; Kim, Hamilton, & Gotlib, 2008). These clinical studies of depression suggest that alterations in white matter volume are associated with the severity of clinical symptoms and with the duration of the disease (Tham et al., 2011). However, it has been argued that the inconsistent results regarding white matter volume should be interpreted with caution. Moreover, the reasons for the different results regarding white matter volume may be due to confounding factors in complex clinical studies, such as age, gender, age at onset, antidepressant medication, sample composition, depression severity, various brain areas, and adopted methodology. Clearly, the most direct approach to test whether white matter volume is decreased in depression is to examine white matter volume in the postmortem brain tissue from depressed patients. Investigating changes in white matter in depressed patients would help to further elucidate whether white matter changes play an important role in the etiopathology of depression. However, obtaining the postmortem brains from depressed patients is very difficult. Therefore, in this study, we studied the white matter of brains acquired from an animal model of depression. We subjected adult rats to chronic stress, a vulnerability factor for depression, and subsequently measured changes in the white matter. Most previous studies have used MRI to measure white matter volume, although such imaging measurements are indirect, and artifacts cannot be completely corrected (Scholz, Klein, Behrens, & Johansen-Berg, 2009). Therefore, another well-designed methodology should be adopted to obtain more precise white matter volume measurements in brain regions associated with depression. In this study, to obtain accurate estimates of white matter volume, modern stereological sampling and measuring principles were applied. Our findings demonstrated a significant decrease in white matter volume in rat brains after 28 days of chronic stress. Therefore, stress-induced changes in white matter may be one of the structural bases for stress-induced depressive-like states. However, the exact functional consequence of stress-induced structural changes in the white matter of depressed brains requires further investigation.

Nevertheless, the causes of white matter atrophy in depressed brains remain unknown. The most striking changes in the stress-related rat model of major depressive disorder (MDD) used in this study were reductions in the total volume and total length of myelinated nerve fibers in the white matter. The decrease in white matter volume may be the result of changes in nerve fibers and/or glial cells and/or a loss of extracellular space in the white matter. Previous MRI studies of depression demonstrated that WMHs, which are areas of local demyelination, were increased in depressed subjects (Bae et al., 2006; Banasr & Duman, 2008; O'Brien et al., 1996; Krishnan et al., 2006; Tham et al., 2011). FA in DTI is a measure of tract alignment and integrity. The results of DTI studies indirectly reflect abnormalities of myelinated fibers and myelin sheaths. Using DTI, some researchers have reported abnormalities of myelinated fibers and myelin sheaths in elderly subjects with late-life depression (Sexton, Mackay, & Ebmeier, 2009; Tham et al., 2011). However, other DTI studies reported altered white matter integrity in young depressed subjects (Li et al., 2007; Ma et al., 2007). The previous results indicate that altered white matter integrity may be one of the basic characteristics of depression. However, measurements derived from brain imaging studies are indirect, and the interpretation of such imaging data is complex. Fibers in the white matter cannot be precisely visualized in MRI and DTI scans. Thus, whether imaging measurements of white matter changes reflect demyelination, axonal loss, or another form of white matter disruption remains unknown. There is currently no method available for dividing the white matter into subregions. Therefore, we studied the entire white matter instead of each white matter subregion. Subregion changes in the white matter should be further investigated when a method to define the boundaries of each region becomes available. Modern stereological methods are used to obtain accurate three-dimensional morphometric features, which are

helpful for precisely quantifying white matter parameters (Gundersen et al., 1988). To reveal the underlying reasons for the stress-induced changes in white matter, this study combined transmission electron microscopy and stereological methods to investigate changes in the myelinated fibers in the white matter. To the best of our knowledge, no previous clinical or preclinical studies have described morphometric investigations of myelinated nerve fibers in the white matter of depressed brains. In this study, consistent with the volumetric white matter decrease, the volume and length of myelinated fibers in the white matter were significantly decreased in the CUS rats, suggesting that the white matter shrinkage was likely due to the changes in the myelinated fibers. Notably, we did not find significant differences in the volume density and length density of myelinated fibers in the white matter between the control rats and the CUS rats. We used Cavalier's principle to calculate the entire volume of the white matter. The isector technique was used to ensure all myelinated fibers in the three-dimensional space had an equal probability of being sampled. Then, we multiplied the white matter volume by the myelinated fiber volume density and length density in the white matter to obtain the total volume and length of the myelinated fibers in the white matter. Therefore, our results accurately reflect the amount of the myelinated fibers in the white matter of the entire brain, in addition to density, thus avoiding possible inaccuracy of the density results due to the reference space trap (Braendgaard & Gundersen, 1986).

Our findings demonstrated significant stress-related loss of the total length and total volume of the myelinated fibers in the white matter. To determine the cause of the decreases in myelinated fiber length and volume in the white matter of stressed brains, the myelin sheath ultrastructure of the myelinated fibers in the white matter must be investigated. In this study, we further designed a series of quantitative studies to evaluate the ultramicrostructure of the myelin sheaths in the white matter using modern stereological methods. We examined the myelin sheath volume, axon volume, the mean diameter and perimeter of myelinated fibers. The mean diameter of the myelinated nerve fibers in the white matter was significantly smaller in the CUS group than that in the control group. In addition, we found that the total volume of the myelin sheaths in the white matter in the CUS group was 18.14% lower than that in the control group, which was not significant. However, the total volume of axons in the white matter in the CUS group was 28.27% lower than that in the control group, which was significant. We speculated that no remarkable changes in number of neurons and axons occurred within a four-week period of CUS. However, the cause of the stress-induced decrease in the myelinated fiber axon volume in the white matter remains unknown. One possibility is that the myelinated fibers are demyelinated, which could lead to a decrease in the total axon volume of the myelinated fibers in the white matter; however, unmyelinated fibers were not included in our investigation. This result further supports the idea that chronic stress causes demyelination in the white matter. Moreover, because the myelin sheath volume only contributes a small portion to the myelinated fiber volume, the total volume of the myelinated fibers in the white matter of depressed brains could change significantly while the myelin sheath volume remains unchanged. This result, together with previous findings in this study, further indicates that stress may induce demyelination and/or dysmyelination. The demyelination of myelinated fibers and/or the degeneration of axons and the subsequent breakdown of myelin can lead to decreases in the myelinated fiber length and volume in the white matter of depressed brains. The myelin sheaths around myelinated fibers modulate the impulse conduction velocity through the fibers by fundamentally changing the way impulses are propagated (Nave, 2010). Functionally, white matter integrity provides critical insulation that facilitates axonal conduction by increasing the resistance and lowering the capacitance of the axonal membrane, which allows for faster conduction speeds in myelinated axons compared to unmyelinated axons of the same diameter. Impaired myelinated fiber structure and function can affect neural circuitry, leading to downstream effects related to emotionality in rodents and potentially to mood regulation in humans with depression. Therefore, the deficit in the information conduction of the central nervous system induced by white matter changes in depression may be one of the neural structural bases of mood disorders.

To the best of our knowledge, this study provides the first direct experimental evidence of impaired myelinated fibers in white matter in an animal model of depression. Significant stress-related changes were found in the white matter. These results demonstrated that animals exposed to CUS exhibited behavioral deficits, such as anhedonia, as well as decreases in white matter volume, total volume, and total length and mean diameter of the myelinated fibers in the white matter. These findings extend our understanding of the vital role of white matter in the neurophysiologic mechanisms involved in depression, suggesting that changes in white matter structure and function are specific to chronic stress-induced pathology. Further characterization of the molecular and cellular mechanisms underlying white matter changes and the related signaling pathways should be further investigated.

REFERENCES

Abe, O., Yamasue, H., Kasai, K., Yamada, H., Aoki, S., Inoue, H., … Ohtomo K. (2010). Voxel-based analyses of gray/white matter volume and diffusion tensor data in major depression. *Psychiatry Research*, *181*, 64–70.

Bae, J. N., MacFall, J. R., Krishnan, K. R., Payne, M. E., Steffens, D. C., & Taylor, W. D. (2006). Dorsolateral prefrontal cortex and anterior cingulate cortex white matter alterations in late-life depression. *Biological Psychiatry*, *60*, 1356–1363.

Ballmaier, M., Toga, A. W., Blanton, R. E., Sowell, E. R., Lavretsky, H., Peterson, J., … Kumar, A. (2004). Anterior cingulate, gyrus rectus, and orbitofrontal abnormalities in elderly depressed patients: an MRI-based parcellation of the prefrontal cortex. *The American Journal of Psychiatry*, *161*, 99–108.

Banasr, M., & Duman, R. S. (2008). Glial loss in the prefrontal cortex is sufficient to induce depressive-like behaviors. *Biological Psychiatry*, *64*, 863–870.

Banasr, M., Valentine, G. W., Li, X. Y., Gourley, S. L., Taylor, J. R., & Duman, R. S. (2007). Chronic unpredictable stress decreases cell proliferation in the cerebral cortex of the adult rat. *Biological Psychiatry*, *62*, 496–504.

Bell-McGinty, S., Butters, M. A., Meltzer, C. C., Greer, P. J., Reynolds, C. F. III, & Becker, J. T. (2002). Brain morphometric abnormalities in geriatric depression: Long-term neurobiological effects of illness duration. *The American Journal of Psychiatry*, *159*, 1424-1427.

Berton, O., & Nestler, E. J. (2006). New approaches to antidepressant drug discovery: Beyond monoamines. *Nature Reviews Neuroscience*, *7*, 137–151.

Bondi, C. O., Rodriguez, G., Gould, G. G., Frazer, A., & Morilak, D. A. (2008). Chronic unpredictable stress induces a cognitive deficit and anxiety-like behavior in rats that is prevented by chronic antidepressant drug treatment. *Neuropsychopharmacology*, *33*, 320–331.

Braendgaard, H., & Gundersen, H. J. (1986). The impact of recent stereological advances on quantitative studies of the nervous system. *Journal of Neuroscience Methods*, *18*, 39–78.

Brambilla, P., Nicoletti, M., Sassi, R. B., Mallinger, A. G., Frank, E., Keshavan, M. S., & Soares, J. C. (2004). Corpus callosum signal intensity in patients with bipolar and unipolar disorder. *Journal of Neurology, Neurosurgery, and Psychiatry*, *75*, 221–225.

Cai, X., Kallarackal, A. J., Kvarta, M. D., Goluskin, S., Gaylor, K., Bailey, A. M., … Thompson, S. M. (2013). Local potentiation of excitatory synapses by serotonin and its alteration in rodent models of depression. *Nature Neurosci*, *16*, 464–472.

Christianson, J. P., Paul, E. D., Irani, M., Thompson, B. M., Kubala, K. H., Yirmiya, R., … Maier, S. F. (2008). The role of prior stressor controllability and the dorsal raphe nucleus in sucrose preference and social exploration. *Behavioural Brain Research*, *193*, 87–93.

Couch, Y., Anthony, D. C., Dolgov, O., Revischin, A., Festoff, B., Santos, A. I., … Strekalova, T. (2013). Microglial activation, increased TNF and SERT expression in the prefrontal cortex define stress-altered behaviour in mice susceptible to anhedonia. *Brain, Behavior, and Immunity*, *29*, 136–146.

Czeh, B., Michaelis, T., Watanabe, T., Frahm, J., de Biurrun, G., van Kampen, M., … Fuchs, E. (2001). Stress-induced changes in cerebral metabolites, hippocampal volume, and cell proliferation are prevented by antidepressant treatment with tianeptine. *Proceedings of the National Academy of Sciences of the United States of America*, *98*, 12796–12801.

Dalby, R. B., Chakravarty, M. M., Ahdidan, J., Sorensen, L., Frandsen, J., Jonsdottir, K. Y., … Videbech, P. (2010). Localization of white-matter lesions and effect of vascular risk factors in late-onset major depression. *Psychological Medicine*, *40*, 1389–1399.

Drevets, W. C. (2003). Neuroimaging abnormalities in the amygdala in mood disorders. *Annals of the New York Academy of Sciences*, *985*, 420–444.

Drevets, W. C., Price, J. L., & Furey, M. L. (2008). Brain structural and functional abnormalities in mood disorders: Implications for neurocircuitry models of depression. *Brain Structure & Function*, *213*, 93–118.

Duman, R. S., Heninger, G. R., & Nestler, E. J. (1997). A molecular and cellular theory of depression. *Archives General Psychiatry*, *54*, 597–606.

Duman, R. S., Malberg, J., Nakagawa, S., & D'Sa, C. (2000). Neuronal plasticity and survival in mood disorders. *Biological Psychiatry*, *48*, 732–739.

Frodl, T., Zill, P., Baghai, T., Schule, C., Rupprecht, R., Zetzsche, T., … Meisenzahl, E. M. (2008). Reduced hippocampal volumes associated with the long variant of the tri- and diallelic serotonin transporter polymorphism in major depression. *American Journal of Medical Genetics Part B: Neuropsychiatric Genetics*, *147b*, 1003–1007.

Gundersen, H. J. G. (1977). Notes on the estimation of the numerical density of arbitrary profiles: The edge effect. *Journal of Microscopy*, *111*, 219–223.

Gundersen, H. J., Bendtsen, T. F., Korbo, L., Marcussen, N., Moller, A., Nielsen, K., … West, M. J. (1988). Some new, simple and efficient stereological methods and their use in pathological research and diagnosis. *APMIS*, *96*, 379–394.

Hashimoto, R., Numakawa, T., Ohnishi, T., Kumamaru, E., Yagasaki, Y., Ishimoto, T., … Kunugi, H. (2006). Impact of the DISC1 Ser704Cys polymorphism on risk for major depression, brain morphology and ERK signaling. *Human Molecular Genetics*, *15*, 3024–3033.

Heiden, A., Kettenbach, J., Fischer, P., Schein, B., Ba-Ssalamah, A., Frey, R., … Kasper, S. (2005). White matter hyperintensities and chronicity of depression. *Journal of Psychiatric Research*, *39*, 285–293.

Iosifescu, D. V., Renshaw, P. F., Lyoo, I. K., Lee, H. K., Perlis, R. H., Papakostas, G. I., … Fava, M. (2006). Brain white-matter hyperintensities and treatment outcome in major depressive disorder. *The British Journal of Psychiatry*, *188*, 180–185.

Kieseppa, T., Eerola, M., Mantyla, R., Neuvonen, T., Poutanen, V. P., Luoma, K., … Isometsa, E. (2010). Major depressive disorder and white matter abnormalities: A diffusion tensor imaging study with tract-based spatial statistics. *The Journal of Affective Disorders*, *120*, 240–244.

Kim, M. J., Hamilton, J. P., & Gotlib, I. H. (2008). Reduced caudate gray matter volume in women with major depressive disorder. *Psychiatry Research*, *164*, 114–122.

Krishnan, V., Han, M. H., Graham, D. L., Berton, O., Renthal, W., Russo, S. J., … Nestler, E. J. (2007). Molecular adaptations underlying susceptibility and resistance to social defeat in brain reward regions. *Cell*, *131*, 391–404.

Krishnan, V., & Nestler, E. J. (2008). The molecular neurobiology of depression. *Nature*, *455*, 894–902.

Krishnan, M. S., O'Brien, J. T., Firbank, M. J., Pantoni, L., Carlucci, G., Erkinjuntti, T., … Inzitari, D. (2006). Relationship between periventricular and deep white matter lesions and depressive symptoms in older people. The LADIS study. *International Journal of Geriatric Psychiatry*, *21*, 983–989.

Kumar, A., Gupta, R. C., Albert, T. M., Alger, J., Wyckoff, N., & Hwang, S. (2004). Biophysical changes in normal-appearing white matter and subcortical nuclei in late-life major depression detected using magnetization transfer. *Psychiatry Research*, *130*, 131–140.

Li, L., Ma, N., Li, Z., Tan, L., Liu, J., Gong, G., … Xu, L. (2007). Prefrontal white matter abnormalities in young adult with major depressive disorder: A diffusion tensor imaging study. *Brain Research*, *1168*, 124–128.

Li, C., Yang, S., Chen, L., Lu, W., Qiu, X., Gundersen, H. J., & Tang, Y. (2009). Stereological methods for estimating the myelin sheaths of the myelinated fibers in white matter. *The Anatomical Record (Hoboken)*, *292*, 1648–1655.

Ma, N., Li, L., Shu, N., Liu, J., Gong, G., He, Z., … Jiang, T. (2007). White matter abnormalities in first-episode, treatment-naive young adults with major depressive disorder. *The American Journal of Psychiatry*, *164*, 823–826.

Magarinos, A. M., Deslandes, A., & McEwen, B. S. (1999). Effects of antidepressants and benzodiazepine treatments on the dendritic structure of CA3 pyramidal neurons after chronic stress. *European Journal of Pharmacology*, *371*, 113–122.

Manji, H. K., Drevets, W. C., & Charney, D. S. (2001). The cellular neurobiology of depression. *Nature Medicine*, *7*, 541–547.

Manji, H. K., Quiroz, J. A., Sporn, J., Payne, J. L., Denicoff, K., N, A. G., … Charney, D. S. (2003). Enhancing neuronal plasticity and cellular resilience to develop novel, improved therapeutics for difficult-to-treat depression. *Biological Psychiatry*, *53*, 707–742.

McEwen, B. S. (2000). Effects of adverse experiences for brain structure and function. *Biological Psychiatry*, *48*, 721–731.

Nave, K. A. (2010). Myelination and support of axonal integrity by glia. *Nature*, *468*, 244–252.

Neumeister, A., Wood, S., Bonne, O., Nugent, A. C., Luckenbaugh, D. A., Young, T., … Drevets, W. C. (2005). Reduced hippocampal volume in unmedicated, remitted patients with major depression versus control subjects. *Biological Psychiatry*, *57*, 935–937.

Nyengaard, J. R., & Gundersen, H. J. G. (1992). The isector: A simple and direct method for generating isotropic, uniform random sections from small specimens. *Journal of Microscopy*, *165*, 427–431.

O'Brien, J. T., Ames, D., Schweitzer, I., Colman, P., Desmond, P., & Tress, B. (1996). Clinical and magnetic resonance imaging correlates of hypothalamic-pituitary-adrenal axis function in depression and Alzheimer's disease. *The British Journal of Psychiatry*, *168*, 679–687.

Papakostas, G. I., Iosifescu, D. V., Renshaw, P. F., Lyoo, I. K., Lee, H. K., Alpert, J. E., … Fava, M. (2005). Brain MRI white matter hyperintensities and one-carbon cycle metabolism in non-geriatric outpatients with major depressive disorder (Part II). *Psychiatry Research*, *140*, 301–307.

Pittenger, C., & Duman, R. S. (2008). Stress, depression, and neuroplasticity: A convergence of mechanisms. *Neuropsychopharmacology*, *33*, 88–109.

Santarelli, L., Saxe, M., Gross, C., Surget, A., Battaglia, F., Dulawa, S., … Hen, R. (2003). Requirement of hippocampal neurogenesis for the behavioral effects of antidepressants. *Science*, *301*, 805–809.

Schmidt, H. D., & Duman, R. S. (2007). The role of neurotrophic factors in adult hippocampal neurogenesis, antidepressant treatments and animal models of depressive-like behavior. *Behavioural Pharmacology*, *18*, 391–418.

Scholz, J., Klein, M. C., Behrens, T. E., & Johansen-Berg, H. (2009). Training induces changes in white-matter architecture. *Nature Neuroscience*, *12*, 1370–1371.

Seney, M. L., Walsh, C., Stolakis, R., & Sibille, E. (2012). Neonatal testosterone partially organizes sex differences in stress-induced emotionality in mice. *Neurobiology of Disease*, *46*, 486–496.

Sexton, C. E., Mackay, C. E., & Ebmeier, K. P. (2009). A systematic review of diffusion tensor imaging studies in affective disorders. *Biological Psychiatry*, *66*, 814–823.

Sheline, Y. I., Price, J. L., Vaishnavi, S. N., Mintun, M. A., Barch, D. M., Epstein, A. A., … McKinstry, R. C. (2008). Regional white matter hyperintensity burden in automated segmentation distinguishes late-life depressed subjects from comparison subjects matched for vascular risk factors. *The American Journal of Psychiatry*, *165*, 524–532.

Sheline, Y. I., Wang, P. W., Gado, M. H., Csernansky, J. G., & Vannier, M. W. (1996). Hippocampal atrophy in recurrent major depression. *Proceedings of the National Academy of Sciences of the United States of America*, *93*, 3908–3913.

Steingard, R. J., Renshaw, P. F., Hennen, J., Lenox, M., Cintron, C. B., Young, A. D., … Yurgelun-Todd, D. A. (2002). Smaller frontal lobe white matter volumes in depressed adolescents. *Biological Psychiatry*, *52*, 413–417.

Strekalova, T., Gorenkova, N., Schunk, E., Dolgov, O., & Bartsch, D. (2006). Selective effects of citalopram in a mouse model of stress-induced anhedonia with a control for chronic stress. *Behavioural Pharmacology*, *17*, 271–287.

Tang, Y., & Nyengaard, J. R. (1997). A stereological method for estimating the total length and size of myelin fibers in human brain white matter. *Journal of Neuroscience Methods*, *73*, 193–200.

Tang, Y., Nyengaard, J. R., Pakkenberg, B., & Gundersen, H. J. (1997). Age-induced white matter changes in the human brain: A stereological investigation. *Neurobiology of Aging*, *18*, 609–615.

Taylor, W. D., MacFall, J. R., Payne, M. E., McQuoid, D. R., Provenzale, J. M., Steffens, D. C., & Krishnan, K. R. (2004). Late-life depression and microstructural abnormalities in dorsolateral prefrontal cortex white matter. *The American Journal of Psychiatry*, *161*, 1293–1296.

Tham, M. W., Woon, P. S., Sum, M. Y., Lee, T. S., & Sim, K. (2011). White matter abnormalities in major depression: Evidence from post-mortem, neuroimaging and genetic studies. *The Journal of Affective Disorders*, *132*, 26–36.

Weber, K., Giannakopoulos, P., Delaloye, C., de Bilbao, F., Moy, G., Moussa, A., … Canuto, A. (2010). Volumetric MRI changes, cognition and personality traits in old age depression. *The Journal of Affective Disorders*, *124*, 275–282.

Willner, P. (2005). Chronic mild stress (CMS) revisited: Consistency and behavioural-neurobiological concordance in the effects of CMS. *Neuropsychobiology*, *52*, 90–110.

Willner, P., Towell, A., Sampson, D., Sophokleous, S., & Muscat, R. (1987). Reduction of sucrose preference by chronic unpredictable mild stress, and its restoration by a tricyclic antidepressant. *Psychopharmacology (Berl)*, *93*, 358–364.

Wong, M. L., & Licinio, J. (2001). Research and treatment approaches to depression. *Nature Reviews Neuroscience*, *2*, 343–351.

Xiu, Y., Kong, X. R., Zhang, L., Qiu, X., Gao, Y., Huang, C. X., … Tang, Y. (2015). The myelinated fiber loss in the corpus callosum of mouse model of schizophrenia induced by MK-801. *Journal of Psychiatric Research*, *63*, 132–140.

Yang, S., Li, C., Lu, W., Zhang, W., Wang, W., & Tang, Y. (2009). The myelinated fiber changes in the white matter of aged female Long-Evans rats. *Journal of Neuroscience Research*, *87*, 1582–1590.

How to cite this article: Gao Y, Ma J, Tang J, Liang X, Huang C, Wang S, Chen L, Wang W, Tan C, Chao F, Zhang L, Qiu Q, Luo Y, Xiao Q, Du L, Xiao Q, Tang Y. White matter atrophy and myelinated fiber disruption in a rat model of depression. *J. Comp. Neurol.* 2017; 525:1922–1933. https://doi.org/10.1002/cne.24178.